



**Mechanical, Thermal And Electrical Properties  
Of ABS Copper Zinc Ferrite Polymer Composites  
Fabricated Using 3D Printer Compositing Technique**

by

**KHAIRUL AMALI HAMZAH  
(1440411526)**

A thesis submitted in fulfillment of the requirements for the degree of  
Doctor of Philosophy

**School of Materials Engineering  
UNIVERSITI MALAYSIA PERLIS**

2020

## ACKNOWLEDGMENT

My greatest gratitude I express to Allah for giving me strength and spirit to complete my study.

First and foremost, I would like to express my gratitude to my supervisor, Assoc. Prof. Dr. Yeoh Cheow Keat for giving me the opportunity and privilege to work under his supervision. I appreciate all his contributions of time, ideas, knowledge and support for my study. His good advice was very helpful in my research as he has very strong and good knowledge and fundamental in this area of research. I also want to thank my co-supervisor, Assoc. Prof. Dr. Mazlee Mohd Noor for his advice and support.

My special thanks to my beloved family for their endless love and support. I really appreciate their time and money. They always give me lots of encouragement and concern in my study. They will always be with me during good and bad times.

I would like to express my sincere gratitude to the lectures and staff of the School of Materials Engineering, UniMAP for giving me full cooperation, support and also for providing me the proper tools and equipment.

Finally, I would like to give my special thanks to the Malaysia Ministry of Higher Education for financing me with MyBrain 15 Sponsorship Programme (MyPhD). Without their sponsor it would not be possible for me to complete my research. My special acknowledgement for Fundamental Research Grant Scheme (FRGS) under a grant number of FRGS/1/2018/TK05/UNIMAP/02/14 from the Ministry of Education Malaysia for their funding on my research project.

## TABLE OF CONTENTS

	<b>PAGE</b>
<b>DECLARATION OF THESIS</b>	<b>i</b>
<b>ACKNOWLEDGMENT</b>	<b>ii</b>
<b>TABLE OF CONTENTS</b>	<b>iii</b>
<b>LIST OF TABLES</b>	<b>vii</b>
<b>LIST OF FIGURES</b>	<b>viii</b>
<b>LIST OF ABBREVIATIONS</b>	<b>xiii</b>
<b>LIST OF SYMBOLS</b>	<b>xiv</b>
<b>ABSTRAK</b>	<b>xv</b>
<b>ABSTRACT</b>	<b>xvi</b>
<b>CHAPTER 1 : INTRODUCTION</b>	<b>1</b>
1.1 Introduction	1
1.2 Background of Research	2
1.3 Problem Statement	4
1.4 Objective of Research	6
1.5 Scope of Research	6
1.6 Thesis Layout	8
<b>CHAPTER 2 : LITERATURE REVIEW</b>	<b>11</b>
2.1 Introduction	11
2.2 Additive Manufacturing	11
2.3 Important Parameter of 3D Printing	13

2.3.1	Effect of Raster Angle on Printed Specimen	13
2.3.2	Effect of Infill Density on Printed Specimen	16
2.4	Conductive Polymer Composites	17
2.4.1	Thermally Conductive but Electrically Insulative Polymer	19
2.5	Thermally Conductive but Electrically Insulative Filler	20
2.6	Application of Thermally Conductive but Electrically Insulative Polymer	26
2.7	Effect of Filler Loading on Printed Specimen	27
2.8	Summary	29
<b>CHAPTER 3 : METHODOLOGY</b>		<b>32</b>
3.1	Introduction	32
3.2	Raw Materials	34
3.3	Filler Preparation	34
3.4	Preparation of Control Specimen	36
3.5	Preparation of Composites specimen	36
3.6	Testing and Characterization	39
3.6.1	Mechanical Properties	39
3.6.2	Dynamic Mechanical Properties	40
3.6.3	Thermal Analysis	40
3.6.4	Electrical Conductivity	42
3.6.5	Density Analysis	43
3.6.6	Microstructure Analysis	44
3.6.7	Phase Identification Analysis	44
<b>CHAPTER 4 : RESULT AND DISCUSSION</b>		<b>45</b>
4.1	Introduction	45
4.2	Characterization of ZnFe <sub>2</sub> O <sub>4</sub>	45
4.2.1	X-Ray Diffraction of ZnFe <sub>2</sub> O <sub>4</sub>	45

4.2.2	Thermal Gravimetric Analysis of ABS-ZnFe <sub>2</sub> O <sub>4</sub> Composites	46
4.3	Effect of Process Parameter on Properties of ABS	48
4.3.1	Effect of Raster Angle on Mechanical Properties of ABS-ZnFe <sub>2</sub> O <sub>4</sub> Composites	48
4.3.2	Effect of Raster Angle on Dynamic Mechanical Properties of ABS-ZnFe <sub>2</sub> O <sub>4</sub> Composites	58
4.3.3	Effect of Raster Angle on Thermal Conductivity of ABS-ZnFe <sub>2</sub> O <sub>4</sub> Composites	61
4.3.4	Effect of Raster Angle on Electrical Conductivity of ABS-ZnFe <sub>2</sub> O <sub>4</sub> Composites	63
4.3.5	Effect of Infill Density on Mechanical Properties of ABS-ZnFe <sub>2</sub> O <sub>4</sub> Composites	64
4.3.6	Effect of Infill Density on Dynamic Mechanical Properties of ABS-ZnFe <sub>2</sub> O <sub>4</sub> Composites	76
4.3.7	Effect of Infill Density on Thermal Conductivity of ABS-ZnFe <sub>2</sub> O <sub>4</sub> Composites	78
4.3.8	Effect of Infill Density on Electrical Conductivity of ABS-ZnFe <sub>2</sub> O <sub>4</sub> Composites	81
4.3.9	Summary	82
4.4	Effect of Filler Loading on The Properties of ABS-ZnFe <sub>2</sub> O <sub>4</sub> Composites	83
4.4.1	Effect of Filler Loading on Mechanical Properties of ABS-ZnFe <sub>2</sub> O <sub>4</sub> Composites	83
4.4.2	Effect of Filler Loading on Dynamic Mechanical Properties of ABS-ZnFe <sub>2</sub> O <sub>4</sub> Composites	91
4.4.3	Effect of Filler Loading on Thermal Conductivity of ABS-ZnFe <sub>2</sub> O <sub>4</sub> Composites	94
4.4.4	Effect of Filler Loading on Electrical Conductivity of ABS-ZnFe <sub>2</sub> O <sub>4</sub> Composites	95
4.4.5	Summary	97
4.5	Characterization of Cu <sub>(x)</sub> Zn <sub>(1-x)</sub> Fe <sub>2</sub> O <sub>4</sub>	98

4.6	Effect of Different Stoichiometry of Filler on Properties of ABS-Cu <sub>(x)</sub> Zn <sub>(1-x)</sub> Fe <sub>2</sub> O <sub>4</sub> Composites	99
4.6.1	Effect of Different Stoichiometry of Filler on Mechanical Properties of ABS-Cu <sub>(x)</sub> Zn <sub>(1-x)</sub> Fe <sub>2</sub> O <sub>4</sub> Composites	99
4.6.2	Effect of Different Stoichiometry of Filler on Dynamic Mechanical of ABS-Cu <sub>(x)</sub> Zn <sub>(1-x)</sub> Fe <sub>2</sub> O <sub>4</sub> Composites	105
4.6.3	Effect of Different Stoichiometry of Filler on Thermal Conductivity of ABS-Cu <sub>(x)</sub> Zn <sub>(1-x)</sub> Fe <sub>2</sub> O <sub>4</sub> Composites	108
4.6.4	Effect of Different Stoichiometry of Filler on Electrical Conductivity of ABS-Cu <sub>(x)</sub> Zn <sub>(1-x)</sub> Fe <sub>2</sub> O <sub>4</sub> Composites	109
4.6.5	Summary	110
<b>CHAPTER 5 : CONCLUSION AND RECOMMENDATION</b>		<b>112</b>
5.1	Conclusion	112
5.2	Recommendation	115
<b>REFERENCES</b>		<b>116</b>
<b>APPENDIX A</b>		<b>129</b>
<b>APPENDIX B</b>		<b>141</b>
<b>APPENDIX C</b>		<b>144</b>
<b>LIST OF PUBLICATION</b>		<b>150</b>

## LIST OF TABLES

	<b>PAGE</b>
Table 3-1 Properties of Fe <sub>2</sub> O <sub>3</sub> , ZnO and CuO	34
Table 3-2 Printer setup	37
Table 4-1 Speed of motor dispenser	48

@This item is protected by original copyright

## LIST OF FIGURES

	<b>PAGE</b>	
Figure 1.1	Project flow chart	8
Figure 2.1	Image of (a) 3D printer MendelMax 1.5 and (b) part fabricated using a 3D printer	13
Figure 2.2	Effect of raster angle with subjected to tension load (Mohamed et al. 2016)	16
Figure 2.3	Image of different infill density; (a) 20%, (b) 50% and (c) 100% (Fernandez-Vicente et al., 2016)	17
Figure 3.1	Project flow chart	33
Figure 3.2	SEM image of filler (a) before and (b) after precoat	35
Figure 3.3	Modified 3D printer (Reprap MendelMax 1.5)	37
Figure 3.4	Closed up image of printing process	38
Figure 3.5	Specimen dimensions	38
Figure 3.6	Printed specimen at different raster angles (a) $90^{\circ}$ , (b) $45^{\circ}$ and (c) $0^{\circ}$	39
Figure 3.7	The difference of infill density (a) 50%, (b) 75% and (c) 100%	39
Figure 3.8	Thermal conductivity setup (enclosed liquid cooling system)	41
Figure 3.9	(a) Electrical conductivity setup, (b) close up of specimen holder and (c) Electrical conductivity specimen dimension	43
Figure 4.1	Diffractiongram of $ZnFe_2O_4$ samples sintered at different temperature	46

Figure 4.2	Thermograph of ABS-ZnFe <sub>2</sub> O <sub>4</sub> composites at different filler loading	47
Figure 4.3	Tensile strength of ABS-ZnFe <sub>2</sub> O <sub>4</sub> composite at different raster angle and filler loading	49
Figure 4.4	Schematic diagram between filler and raster angle interaction	51
Figure 4.5	Elongation at break of ABS-ZnFe <sub>2</sub> O <sub>4</sub> composite at different raster angle and filler loading	52
Figure 4.6	Young's modulus of ABS-ZnFe <sub>2</sub> O <sub>4</sub> composite at different raster angle and filler loading	54
Figure 4.7	Rockwell Hardness of ABS-ZnFe <sub>2</sub> O <sub>4</sub> composite at different raster angles and filler loadings	56
Figure 4.8	Density of ABS-ZnFe <sub>2</sub> O <sub>4</sub> composite at different raster angles and filler loadings	58
Figure 4.9	Storage modulus of ABS with different raster angle	60
Figure 4.10	Schematic diagram of dynamic mechanic of specimen with different raster angle; (a) 0°, (b) 90° and (c) 45°	60
Figure 4.11	Tan δ of ABS at different raster angle	61
Figure 4.12	Thermal conductivity of ABS-ZnFe <sub>2</sub> O <sub>4</sub> composite at different raster angles and filler loadings	62
Figure 4.13	Electrical conductivity of ABS-ZnFe <sub>2</sub> O <sub>4</sub> composite at different raster angles and filler loadings	64
Figure 4.14	Tensile strength of ABS-ZnFe <sub>2</sub> O <sub>4</sub> composite at different infill density and filler loadings	65
Figure 4.15	Fracture surface of ABS specimen at (a) 50%, (b) 75%, and (c) 100% of infill density	67

Figure 4.16	Elongation at break of ABS-ZnFe <sub>2</sub> O <sub>4</sub> composite at different infill density and filler loadings	68
Figure 4.17	Young's modulus of ABS-ZnFe <sub>2</sub> O <sub>4</sub> composite at different infill density and filler loadings	70
Figure 4.18	Schematic diagram of filler and matrix interaction subjected to infill density	71
Figure 4.19	Fracture surface of ABS-ZnFe <sub>2</sub> O <sub>4</sub> composites	72
Figure 4.20	Hardness of ABS-ZnFe <sub>2</sub> O <sub>4</sub> composites at different infill density and filler loadings	73
Figure 4.21	Density of ABS-ZnFe <sub>2</sub> O <sub>4</sub> composite at different infill density and filler loading	75
Figure 4.22	Storage modulus of ABS at different infill density	77
Figure 4.23	Tan $\delta$ of ABS at different fill density	78
Figure 4.24	Thermal conductivity of ABS-ZnFe <sub>2</sub> O <sub>4</sub> composite at different infill density and filler loading	79
Figure 4.25	Electrical conductivity of ABS-ZnFe <sub>2</sub> O <sub>4</sub> composite at different infill density and filler loading	81
Figure 4.26	Tensile strength of ABS-ZnFe <sub>2</sub> O <sub>4</sub> composite at different filler loading	84
Figure 4.27	SEM image of fracture surface of printed composites specimen; (a) unfilled ABS, (b) ABS with 8 wt% ZnFe <sub>2</sub> O <sub>4</sub> , (c) ABS with 11 wt% ZnFe <sub>2</sub> O <sub>4</sub> and (d) ABS with 14 wt% ZnFe <sub>2</sub> O <sub>4</sub>	85
Figure 4.28	Young's modulus of ABS-ZnFe <sub>2</sub> O <sub>4</sub> composite at different filler loading	87

Figure 4.29	Elongation at break of ABS-ZnFe <sub>2</sub> O <sub>4</sub> composite at different filler loading	88
Figure 4.30	Hardness of ABS-ZnFe <sub>2</sub> O <sub>4</sub> composite at different filler loading	89
Figure 4.31	Density of ABS-ZnFe <sub>2</sub> O <sub>4</sub> composite at different filler loading	91
Figure 4.32	Storage modulus of ABS-ZnFe <sub>2</sub> O <sub>4</sub> composite at different filler loading	92
Figure 4.33	Tan δ of ABS-ZnFe <sub>2</sub> O <sub>4</sub> composite at different filler loading	94
Figure 4.34	Thermal conductivity of ABS-ZnFe <sub>2</sub> O <sub>4</sub> composite at different filler loading	95
Figure 4.35	Electrical conductivity of ABS-ZnFe <sub>2</sub> O <sub>4</sub> composite at different filler loading	97
Figure 4.36	XRD pattern of Cu <sub>(x)</sub> Zn <sub>(1-x)</sub> Fe <sub>2</sub> O <sub>4</sub> formation	98
Figure 4.37	Tensile strength of ABS-Cu <sub>(x)</sub> Zn <sub>(1-x)</sub> Fe <sub>2</sub> O <sub>4</sub> composite at different filler stoichiometry	100
Figure 4.38	Elongation at break of ABS-Cu <sub>(x)</sub> Zn <sub>(1-x)</sub> Fe <sub>2</sub> O <sub>4</sub> composite at different filler stoichiometry	101
Figure 4.39	Young's modulus of ABS-Cu <sub>(x)</sub> Zn <sub>(1-x)</sub> Fe <sub>2</sub> O <sub>4</sub> composite at different filler stoichiometry	102
Figure 4.40	Hardness of ABS-Cu <sub>(x)</sub> Zn <sub>(1-x)</sub> Fe <sub>2</sub> O <sub>4</sub> composite at different filler stoichiometry	104
Figure 4.41	Density of ABS-Cu <sub>(x)</sub> Zn <sub>(1-x)</sub> Fe <sub>2</sub> O <sub>4</sub> composite at different filler stoichiometry	105
Figure 4.42	Storage modulus of ABS-Cu <sub>(x)</sub> Zn <sub>(1-x)</sub> Fe <sub>2</sub> O <sub>4</sub> composite at different filler stoichiometry	106

Figure 4.43	Tan $\delta$ of ABS- $\text{Cu}_{(x)}\text{Zn}_{(1-x)}\text{Fe}_2\text{O}_4$ at different filler stoichiometry	107
Figure 4.44	Thermal conductivity of ABS- $\text{Cu}_{(x)}\text{Zn}_{(1-x)}\text{Fe}_2\text{O}_4$ composite at different filler stoichiometry	108
Figure 4.45	Electrical conductivity of ABS- $\text{Cu}_{(x)}\text{Zn}_{(1-x)}\text{Fe}_2\text{O}_4$ composite at different filler stoichiometry	109

@This item is protected by original copyright

## LIST OF ABBREVIATIONS

ABS	Acrylonitrile-Butadiene-Styrene
AM	Additive Manufacturing
CAD	Computer Aided Design
CB	Carbon Black
CF	Carbon Fiber
CNT	Carbon nanotube
$\text{CuFe}_2\text{O}_4$	Copper Ferrite
$\text{CuO}$	Copper Oxide
FDM	Fused Deposition Modeling
$\text{Fe}_2\text{O}_3$	Iron (III) Oxide
LDPE	Low Density Polyester
PC	Polycarbonate
PEEK	Poly-Ether-Ether-Ketone
PLA	Poly-Lactic-Acid
PP	Polypropylene
RPM	Rotation Per Minute
TGA	Thermal Gravimetric Analysis
XRD	X-Ray Diffraction
$\text{ZnFe}_2\text{O}_4$	Zinc Ferrite
$\text{ZnO}$	Zinc Oxide
3D	Three Dimensional

## LIST OF SYMBOLS

$^{\circ}$	Degree
$^{\circ}\text{C}$	Degree Celsius
K	Thermal Conductivity
$\sigma$	Electrical Conductivity
$E'$	Storage Modulus
$\delta$	Delta

@This item is protected by original copyright

## Sifat-Sifat Mekanikal, Termal dan Elektrikal Komposit Polimer ABS Ferit Zink Kuprum Diperbuat Menggunakan Teknik Mengkomposit Pencetak 3D

### ABSTRAK

Kajian ini bertujuan untuk menghasilkan polimer yang mampu mengkonduksikan termal tanpa kekonduksian elektrik yang tinggi menggunakan kaedah baharu penghasilan komposit pencetak 3D. Akrilonitril-butadiena-stirena (ABS) telah digunakan sebagai bahan matrik kerana versatilitinya dan digunakan secara meluas dalam banyak aplikasi. Untuk tujuan kekonduksian, kuprum zinc ferit ( $\text{CuZnFe}_2\text{O}_4$ ) telah dipilih sebagai bahan pengisi kerana sifatnya yang unik yang dapat meningkatkan kekonduksian termal tanpa kekonduksian elektrik yang tinggi. Untuk membuat polimer konduktif ini, pencetak tiga dimensi (pencetak 3D) telah digunakan. Pembuatan komposit menggunakan pencetak 3D semakin mendapat perhatian kerana kelebihannya. Walau bagaimanapun, cabaran utama menggunakan pencetak 3D adalah kekurangan kekuatan mekanik. Oleh itu, penambahan bahan pengisi dan mengubah tetapan pencetak boleh meningkatkan kekuatan mekanik bahan bercetak. Dua tetapan telah digunakan dalam kajian ini iaitu sudut raster ( $0^\circ$ ,  $45^\circ$  dan  $90^\circ$ ) dan ketumpatan isi dalam (50%, 75% dan 100%). Kaedah baharu telah diperkenalkan untuk menghasilkan bahan komposit dengan menggunakan pencetak 3D ini, iaitu teknik penyebaran pengisi semasa proses pencetakan sedang berlaku menggunakan dispenser serbuk. Pengubahsuaian kecil telah dibuat pada pencetak dengan memasang dispenser serbuk. Dispenser dikendalikan pada tiga kelajuan berbeza iaitu kelajuan rendah (1000 rpm), kelajuan sederhana (1400 rpm) dan kelajuan tinggi (1800 rpm) untuk mendapatkan jumlah taburan pengisi yang berbeza. Peratusan pengisi yang ditabur ditentukan menggunakan TGA yang memberi 8% berat untuk kelajuan rendah, 11% berat untuk kelajuan sederhana dan 14% berat untuk kelajuan tinggi. Semua keputusan ujian menunjukkan bahawa penghasilan polimer konduktif terma tetapi insulatif elektrik boleh dibuat dengan menggunakan pencetak 3D menggunakan pengisi yang ditabur. Keputusan menunjukkan peningkatan kekuatan tegangan, peratus pemanjangan, modulus Young dan kekerasan spesimen sebanyak 23%, 66%, 9% dan 21% apabila spesimen dicetak menggunakan sudut raster  $0^\circ$ . Bagi spesimen yang dicetak pada ketumpatan isi dalam 100% menunjukkan peningkatan dalam kekuatan tegangan, modulus dan kekerasan masing-masing adalah sebanyak 17%, 96% dan 64%. Terdapat penurunan dalam peratusan pemanjangan kira-kira 11% pada ketumpatan isi dalam 100%. Walau bagaimanapun, sudut raster dan ketumpatan isi dalam tidak menunjukkan peningkatan ketara dalam kekonduksian terma dan elektrik bahan bercetak. Kira-kira 724% peningkatan kekonduksian terma dan kenaikan sedekad dalam kekonduksian elektrik selepas penambahan dengan penguat 14% wt. Sifat mekanik meningkat sebanyak 118% untuk kekuatan tegangan, 22% untuk modulus Young dan 342% untuk nilai kekerasan selepas penambahan 14 wt% pengisi. Tidak terdapat perubahan ketara dalam sifat mekanikal apabila stoikiometri pengisi diubah. Walau bagaimanapun, kenaikan 63% terhadap kekonduksian terma ditemui dalam spesimen dengan stoikiometri pengisi ditingkatkan dari  $x = 0$  hingga  $x = 1$ .

## Mechanical, Thermal and Electrical Properties of ABS Copper Zinc Ferrite Polymer Composites Fabricated Using 3D Printer Compositing Technique

### ABSTRACT

This study aims to produce polymers that capable of thermally conductive but low electrical conductivity using new fabrication compositing technique of 3D printer. Acrylonitrile-butadiene-styrene (ABS) has been used as a matrix due to its versatility and widely used in many applications. For thermal conduction purposes, copper zinc ferrite ( $\text{CuZnFe}_2\text{O}_4$ ) have been selected as filler due to their unique properties which can improve thermal conductivity but has low electrical conductivity. To fabricate this conductive polymer, a three-dimensional printer (3D printer) was used. Fabrication of composites using 3D printers is gaining attention due to their advantages. However, the main challenge of using 3D printers is the lack of mechanical strength of the printed part. Therefore, the addition of filler material and varying the printer setting may increase the mechanical strength of the printed material. Two settings were used in this study which are raster angles ( $0^\circ$ ,  $45^\circ$  and  $90^\circ$ ) and infill density (50%, 75% and 100%). New methods have been introduced to produce composite materials using this 3D printer, which is the distributing of filler during the printing process using powder dispenser. Small modification has been made on the printer by installing powder dispenser. The dispenser was operated at three different speeds which are low speed (1000 rpm), medium speed (1400 rpm) and high speed (1800 rpm) to obtain different dispensed amounts of filler. The percentage of dispensed filler was determined using TGA which give 8 wt% for low speed, 11 wt% for medium speed and 14 wt% for high speed. All test results show that the production of thermally conductive, but electrically insulative polymers can be made using 3D printers utilizing dispensed filler. The results showed an increase in tensile strength, percentage of elongation at break, Young's modulus and hardness of the specimens by 23%, 66%, 9% and 21% respectively when the specimens were printed using raster angles  $0^\circ$ . For specimens printed at 100% infill density showed an increase in tensile strength, Young's modulus and hardness values were 17%, 96% and 64%, respectively. There was a decrease in the percentage of elongation about 11% at 100% infill density. However, the raster angle and infill density do not show insignificant increase in thermal and electrical conductivity of the printed material. Approximately 724% increase in thermal conductivity and a decade increment in electrical conductivity after addition with a 14 wt% filler. The increase in mechanical properties and dynamic mechanical properties also increased by 118% for tensile strength, 22% for Young's modulus and 342% for hardness value after addition of 14 wt% filler. No significant changes were noted in mechanical and dynamic mechanical properties when the stoichiometric of reinforcer is changed. However, a 63% increase in thermal conductivity was found in specimens with a filler stoichiometry is increased from  $x = 0$  to  $x=1$ .

@This item is protected by original copyright

## CHAPTER 1 : INTRODUCTION

### 1.1 Introduction

3D printing is additive manufacturing (AM) technology used to fabricate the end product by depositing material layer by layer. Previous studies have proved the ability of 3D printed to manufacture the end product. Nevertheless, the research also found that the part produced by the 3D printer is mechanically weak. The drawback has shown that the process parameter of the machine can be one of the solutions to improve the strength of the fabricated product. Instead of the process parameters of the machine, the addition of filler is another alternative to improve the properties of the printed materials. Previously, improving the mechanical properties of the printed part of the 3D printer has been done by altering the process parameter. However, in some cases like to constructing a thermally conductive but electrically insulative polymer composites component acquire another way to create the properties which unable to be fabricated by altering the process parameters. Therefore, the addition of filler that has thermally conductive but electrically insulative properties may be one of the solutions. Ceramic ferrite is one of the fillers that match to the requirement of fabricating specimen with those properties. The thermally conductive but electrically insulative polymer is the unique properties that are widely used in electronic and microelectronic devices (X. Zhang et al., 2017). The reason for electrical insulative is for safety reasons from the electrical leakage while the reason of thermally conductive is to prevent component damages (X. Zhang et al., 2017). This research attempts to fabricate a thermally conductive but electrically insulative polymer using a 3D printing technique. This project also has introduced an in-situ technique to obtain composites specimen compared to the previous technique that used a conductive

filament. Simple modification has been done on the 3D printer to simplify the fabrication process of the composite specimen. Acrylonitrile-butadiene-styrene (ABS) was used as a polymer matrix and filled with ceramic ferrite filler to increase the properties of the printed part.

## **1.2 Background of Research**

3D printing is an alternative method of fabricating a prototype component. Many researches were done to improve the properties of the printed component. Previous study has shown that the mechanical properties can be improved by altering the process parameters. However, process parameters are not improving other properties such as thermal and electrical conductivity due to the insulative behaviour of the polymer. The addition of filler is a good way to improve these properties. Previously, the composites specimen prepared using a 3D printer was by using a composite filament as done by S. Dul et al., 2016 to study the properties of ABS-graphene nanocomposite using fused deposition modelling. They have prepared the filament by compounding the ABS and graphene before go to the next stage which is filament extrusion (Dul, Fambri, & Pegoretti, 2016). Extra work is needed to prepare a composite filament. The selected filler is added into the polymer and made into filament before use to be printed as a part.

The 3D printing technique is found in 1980 by Scott Crump (Rankouhi, Javadpour, Delfanian, & Letcher, 2016). The advantages of 3D printing are printing complex geometry, operating at low temperature, and lower setup and operation cost (Berman, 2012; Huang, Liu, & Mokasdar, 2013; Jain & Kuthe, 2013; Birtchnell & Urry, 2013). The 3D printer works by depositing molten material layer upon layer until the 3D

shape is formed (Rankouhi et al., 2016). 3D printing technique starts with design 3D drawing in computer-aided-design (CAD) software. The CAD file was then converted to triangulation language (STL). In this format, the 3D drawing was sliced into thin layers. Every slice contains geometric information, which is transmitted to the 3D printer in sequence. Finally, the printer constructs each layer on top of another, based on received data (P. Feng, Meng, Chen, & Ye, 2015).

Acrylonitrile-Butadiene-Styrene (ABS) is widely used in various applications such as electronic, automotive and many more (Olivera, Muralidhara, Venkatesh, Gopalakrishna, & Vivek, 2016; F. Wang, Zhang, Zhang, Hong, Kumar, & Xie, 2015; J. Feng, Carpanese, & Fina, 2016). ABS have good mechanical properties in a group of thermoplastics (Olivera et al., 2016; J. Feng, Carpanese, et al., 2016). ABS have a unique characteristic such as easy to process in many ways and require low temperature to process. ABS is also categorized as an inexpensive material with good quality (Olivera et al., 2016a).

Ceramic is a multifunctional filler that has good hardness and thermal properties and low electrical conductivity (Bardhan, Ghosh, Mitra, Das, Mukherjee, & Chattopadhyay, 2010). Hence, by incorporating this filler into ABS it may increase the mechanical properties while maintaining low electrical conductivity of ABS. Currently, ferrites are widely used as a filler to improve the thermally conductive but low electrical conductivity properties of the material. Copper Zinc Ferrite ( $\text{CuZnFe}_2\text{O}_4$ ) is one of the materials that can be used to modify electrical and optical properties (Bardhan et al., 2010). The structure of  $\text{ZnFe}_2\text{O}_4$  is normally in spinel structure. Besides,  $\text{ZnFe}_2\text{O}_4$  structure also can be found in cubic closed-packed, tetrahedral and octahedral (Raeisi

Shahraki, Ebrahimi, Seyyed Ebrahimi, & Masoudpanah, 2012). By adding ferrites into the polymer matrix, it may increase the strength and thermal conductivity but low electrical conductivity of the polymer.

This study aims to fabricate thermally polymer composites using a modified 3D printer. The composites specimen was obtained by using filler dispensed technique. The properties of the printed part were improved by altering the process parameters and the addition of  $\text{CuZnFe}_2\text{O}_4$  filler.

### **1.3 Problem Statement**

Raster angle and infill density are two process parameter that highly effect the mechanical properties of the printed part (Rajpurohit & Dave, 2018)(Fernandez-Vicente, Calle, Ferrandiz, & Conejero, 2016). In this research, raster angle and infill density have been chosen to be studied on how the dispensed filler technique give effect to the properties of printed part and how the technique interact on raster angle and infill density. currently, composites by 3D printer is prepared using a composite filament and print to the desired shape. However, this method is expensive and requires extra work to prepare a composite filament such as compounding and then shaping into the filament wire (Dul et al., 2016) which may increase the fabrication time.

Composites can be used to improve the conductivity of the printed specimen. The conductivity of polymer can be increased by introducing conductive filler into the insulative polymer (Zhu et al., 2017). Thermally conductive but electrically insulating filler like  $\text{CuZnFe}_2\text{O}_4$  is one alternative filler that suits the application. Filler loading also

may give different range of results to the printed specimen. However, filament with different filler loading is difficult to find and required special orders and custom because readymade 3D printer filament unable to control the filler loading as required by these applications which need to be ordered and costly.

Filler selection is the major concern to be considered to improve material properties. Most of the filler could increase the mechanical properties but not all filler has the ability to enhance the conductivity of the polymer such as fibre. As reported by Oqla et al. (2015), fibre provide good insulation properties for conductivity and at the same time promotes good mechanical properties (Al-Oqla, Sapuan, Anwer, Jawaid, & Hoque, 2015). Meanwhile, metal-based filler and carbon-based filler can be used to increase the thermal and electrical conductivity of the polymer. However, metal-based and carbon-based fillers are not suitable in some application such as thermally conductive but electrically resistive material. Previous research shows that metal and carbon-based filler increased the conductivity in both ways (Nabilah, Yusuf, Bakar, & Sahari, 2017; Hwang, Reyes, Moon, Rumpf, & Kim, 2015a). Hence, ceramic ferrite filler is another alternative candidate of filler that match with the thermally conductive but electrically insulative application. According to a previous study ceramic ferrite filler has unique properties to increase thermal conductivity but low electrical conductivity and increase the mechanical properties of composites (Essabir, Raji, Essassi, Rodrigue, & Bouhfid, 2017). However, each of ceramic ferrite filler or combination of them may give different results due to different intrinsic properties of each. So, it is crucial to study the effect of different composition or stoichiometry on the properties of the printed part.

## 1.4 Objective of Research

Several objectives have been set to ensure that the purpose of the study does not deviate. The objectives are as follows:

1. To find the effect of processing parameters of 3D printer which are raster angle and infill density on the mechanical properties, thermal and electrical conductivity of ABS composites.
2. To determine the effect of filler loading of  $\text{ZnFe}_2\text{O}_4$  on the mechanical properties, thermal and electrical conductivity of ABS composites.
3. To examine the effect of different stoichiometry of  $\text{Cu}_{(x)}\text{Zn}_{(1-x)}\text{Fe}_2\text{O}_4$  filler on the mechanical properties, thermal and electrical conductivity of ABS composites.

## 1.5 Scope of Research

The research works of this study are divided into three main stages which the first stage is the synthesis of filler. The fillers were prepared according to  $\text{Cu}_{(x)}\text{Zn}_{(1-x)}\text{Fe}_2\text{O}_4$  stoichiometry where the x value is 0, 0.25, 0.5, 0.75 and 1. The fillers were synthesized using solid state method (ceramic method) at temperature ranged from 950 °C to 1200 °C. The second stage is specimen preparation. In this stage control (unfilled) specimens and composite specimens were fabricated using 3D printing. The specimen was printed according to raster angle (0°, 45° and 90°) and infill density (50%, 75% and 100%). The

filler was dispensed at different speeds (low speed = 1000 RPM, medium speed = 1400 RPM and high speed = 1800 RPM) during the printing process to obtain composites specimen. The ABS filament was used as a matrix of the composites. The filler loading was determined from the printed specimen at different speeds and the result from that was used in all discussions as weight percent (wt%). The final stage is specimen testing and characterization which meant all specimens underwent mechanical testing, dynamic mechanical testing, thermal and electrical testing. Tensile and hardness test was used as mechanical testing while the density test was used as supporting data. 3-point bending mode was used to performed dynamic mechanical test. Thermal and electrical conductivity was obtained from equations.

Figure 1.1 shows the project flow chart of the research. The flow chart shows that the research works starts by preparing the raw material. This is including filler preparation as a raw material of filler before composites preparation. The second stage is the specimen preparation for both the control specimen and composites specimen. All the parameters such as process parameter (raster angle and infill density), filler loading and different filler stoichiometry are applied at this stage. Lastly, the prepared specimen will be undergone by testing and characterization.

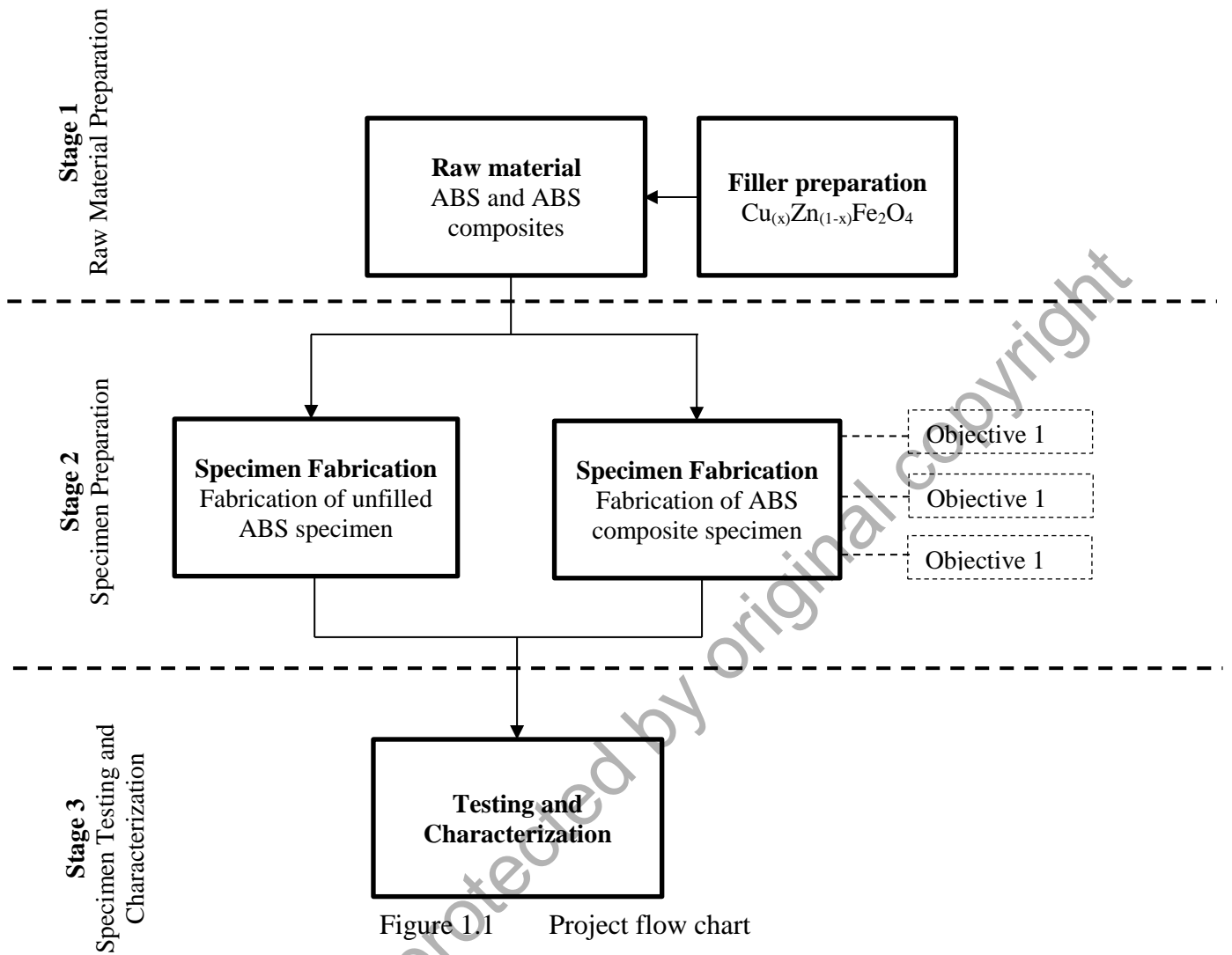


Figure 1.1 Project flow chart

## 1.6 Thesis Layout

This thesis has five chapters that consist of Chapter 1 which is introduction, Chapter 2 literature review, Chapter 3 is the methodology of this project, Chapter 4 is the result and discussion and last chapter which is Chapter 5 that is for conclusion and recommendation.

## Chapter 1: Introduction

This chapter gives some idea about this project generally. The background of research explained the current situation about FDM 3D printer including the problem faced about the 3D printing technique. The objective and scope of research explained what is this project will do to overcome the current situation.

## Chapter 2: Literature Review

Chapter 2 is the review done by the author about the project on previous researchers. This includes the review about 3D printing, polymer composites, thermally conductive but electrically insulative polymer, filler loading, how to prepare the ceramic ferrite filler using solid-state methods and related things about this project. These elements are crucial to be studied to ensure that the project is on point.

## Chapter 3: Methodology

This chapter gives the detail information about this project. This is including the raw material, parameter that involve in this project, also the testing and characterization that has been done to the specimen. This chapter explained how to prepare the  $\text{Cu}_{(x)}\text{Zn}_{(1-x)}\text{Fe}_2\text{O}_4$  filler, the control specimen and composites specimen. This chapter also shows the flow chart of the project to simplify the readers to understand this project.

## Chapter 4: Result and Discussion

This chapter presents the finding collected by the author. This chapter is the analysis and discussion section of the project that covers all important parameter such as the effect of process parameter which is raster angle and infill density, the effect of filler loading and the effect of different filler stoichiometry on the ABS composites properties.

## Chapter 5: Conclusion and Recommendation

Chapter 5 is the section of the overall summary of the findings and analysis of this project that related to the project objective. Additionally, the authors recommend some possible study for future work.

@This item is protected by original copyright

## CHAPTER 2 : LITERATURE REVIEW

### 2.1 Introduction

This chapter will review the basic concept of conductive polymer composites, including the conductive filler, and the application of the conductive polymer. This chapter also will review the additive manufacturing (AM), the working principle of the AM and the concerned parameter on AM processing technique, which was another approach to fabricate a conductive polymer. Lastly, the review will focus on the other important parameter that may affect the fabrication of the conductive polymer such as filler loading and the different filler composition.

### 2.2 Additive Manufacturing

Additive manufacturing is one of several methods used in processing polymer. Under AM technologies, there were several other methods and one of them is three-dimensional printer or 3D printer (Huang et al., 2013; X. Wang, Jiang, Zhou, Gou, & Hui, 2017; Rankouhi et al., 2016). The 3D printer is categorized as rapid prototyping (RP) technology (X. Wang et al., 2017; P. Feng, Meng, & Zhang, 2015; Farzadi, Solati-hashjin, Asadi-eydivand, Azuan, & Osman, 2014) and grouped under Additive Manufacturing. The 3D printer is more like a simplified of fused deposition modelling (FDM) technologies. The concept of fabricating product by AM is by adding the material (Huang et al., 2013; Manu-, 1996; X. Wang et al., 2017) layer upon layer (Huang et al., 2013; Rankouhi et al., 2016; Berman, 2012). It is different from conventional machining processes, which removes material to manufacture a product (Huang et al., 2013). The

3D printer works by depositing molten material onto a heated printing bed (substrate) based on shape design generated by CAD model (Vaezi & Chua, 2011; Rodríguez, Thomas, & Renaud, 2003). The advantages of 3D printing technique are able to print difficult shape, low fabrication cost, material set up and capital cost, tabletop fabrication which contribute to computer integrated manufacturing environment, single-stage manufacture and many more (Vaezi & Chua, 2011; Rodríguez et al., 2003) (Berman, 2012; Rankouhi et al., 2016). Metal, ceramic and polymer are the material suitable to fabricate via this method depending on the technologies and specification of the printer (Utela, Storti, Anderson, & Ganter, 2008). However, in recent decades, the polymer becomes the most material used by 3D printing technology (S. Kumar & Kruth, 2010). Thermoplastic such as ABS, poly-lactic-acid (PLA), and polycarbonate (PC) are usually used in 3D printing (X. Wang et al., 2017; Hwang, Reyes, Moon, Rumpf, & Kim, 2015b; Ning, Cong, Qiu, Wei, & Wang, 2015). 3D printing required low melting temperature to operate thus, thermoplastic is suitable for this technique due to their low melting temperature (Ning et al., 2015; Dul, Fambri, & Pegoretti, 2016). Figure 2.1 (a) shows the example of 3D printer while Figure 2.1 (b) shows an example of a product fabricated by using FDM 3D printing technique.

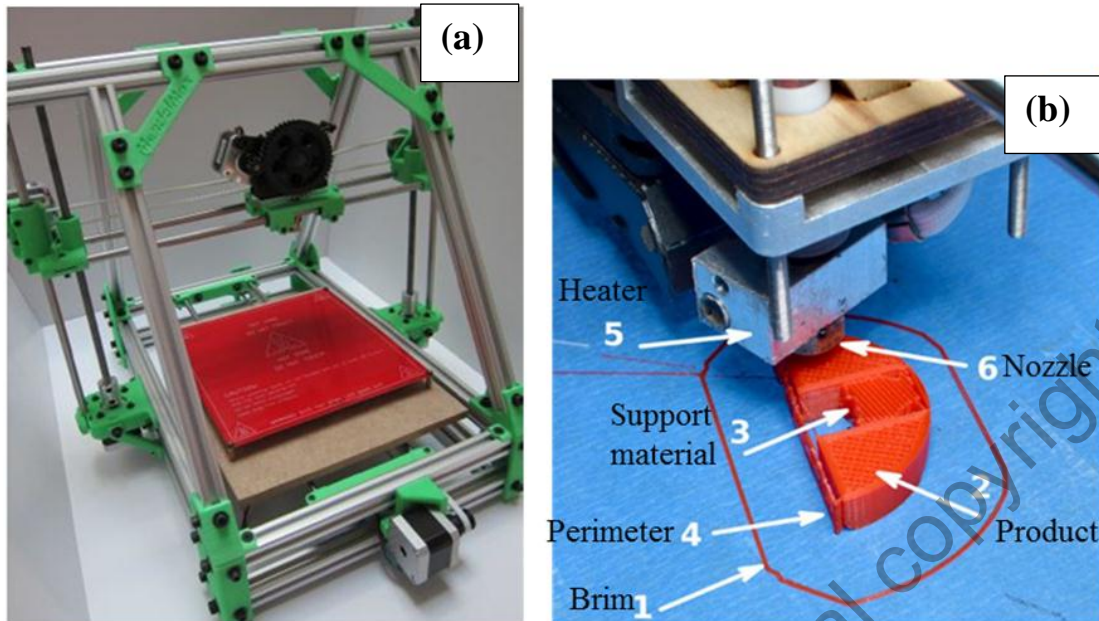


Figure 2.1 Image of (a) 3D printer MendelMax 1.5 and (b) part fabricated using a 3D printer

### 2.3 Important Parameter of 3D Printing

In 3D printing, there are several parameters need to be taken into consideration as these parameters will affect the properties of the printed component especially mechanical properties. Raster orientation, layer height, pattern spacing and infill density are most parameters that have been studied before. The results from previous research have proved that these parameters affect the mechanical properties of the printed part (Rankouhi et al., 2016; Riddick et al., 2016).

#### 2.3.1 Effect of Raster Angle on Printed Specimen

Process parameters are one of the factors that influence the properties of the fabricated product. In this study process parameter is the 3D printer setting. According to Rankouhi et al. (2016), the process parameters that gave the most influence on the

strength of AM product are raster angle, fill density, layer thickness, printing pattern, air gap and operating temperature of the nozzle. They found that the highest tensile strength was obtained in specimens printed in  $0^{\circ}$  orientations while  $90^{\circ}$  orientations show the lowest tensile strength after  $45^{\circ}$  raster orientation. This situation happened because every rasters or layer were pulled laterally to the longitudinal axis that resulted in trans-raster tensile failure. The applied force on specimen printed in  $90^{\circ}$  raster orientation is perpendicular to the raster longitudinal axis which caused inter-raster fusion failure (Rankouhi et al., 2016).

Wu et al. (2015) have studied the effect of layer thickness and raster angle on the mechanical properties of ABS and polyether-ether-ketone (PEEK) prepared via 3D printing technique. The results show that specimens printed at  $0^{\circ}/90^{\circ}$  have the highest tensile strength compared to the specimen with  $30^{\circ}/-60^{\circ}$  and  $45^{\circ}/-45^{\circ}$  raster angle. Low tensile strength happened in the  $30^{\circ}/-60^{\circ}$  and  $45^{\circ}/-45^{\circ}$  raster angle samples because there was a finite angle between the printed microstructural elements and the load direction (Wu, Geng, Li, Zhao, Zhang, & Zhao, 2015).

Another study conducted by Riddick et al. (2016) that examined the effect of raster orientation ( $0^{\circ}$ ,  $45^{\circ}$  and  $90^{\circ}$ ) on the tensile strength of ABS. The tensile strength for samples with  $0^{\circ}$  orientation have the highest tensile strength at 32.60 MPa followed with  $45^{\circ}$  orientation with 27.77 MPa and  $90^{\circ}$  orientation with 15.26 MPa. The highest tensile strength may be due to failure on horizontal edge spanning laterally the orientation of y-axis with breaking of individual raster cross-sections generating overload which permits the fracture to spread across the fracture plane generating a clean surface up to final failure. While the lowest tensile strength was explained happened for specimen

printed in 90° orientation because of rough places on the fracture surface are an indication of the breaking of adhesion between layers (Riddick, Haile, Wahlde, Cole, Bamiduro, & Johnson, 2016).

Cai et al. (2016) investigated the effect of printing orientation on the mechanical properties of ABS. They found that 0° orientation has the highest tensile strength (22.4 MPa) than 45° (20.7 MPa) and 90° (19.0 MPa) orientation. This might be due to when ABS filament printed it creates individual raster align with the loading force direction (Cai, Byrd, Zhang, Schlarman, Zhang, & Golub, 2016).

Zhang et al. (2018) also found a similar finding of an effect of raster orientation on tensile strength. 0° raster orientation shows the highest tensile strength compared to 45° and 90° raster orientation. This is due to stretched polymer molecular orientation according to the printing direction during the printing process. Besides, the presence of void from the process contributed to fabricating a low strength material (W. Zhang et al., 2018).

According to Mohamed et al. (2017), 0° raster angle has the highest tensile strength compared to 45° and 90° of raster angle. This is attributed to the number of rasters, layers, polymer chain molecule and fibre that have to be fracture led to the usage of high stress to fracture. Unlike 0° of raster angle, 45° and 90° required less stress to rupture the specimen. This is because, at 45° and 90° of raster angle, they have a smaller number of raster and easy to fracture (Mohamed, Masood, & Bhowmik, 2017).

Figure 2.2 shows the effect of raster angle subjected to tension load. Higher load required to fracture the  $0^\circ$  raster angle specimen while lower load required to fracture specimen with  $90^\circ$  rasters (Mohamed et al. 2016).

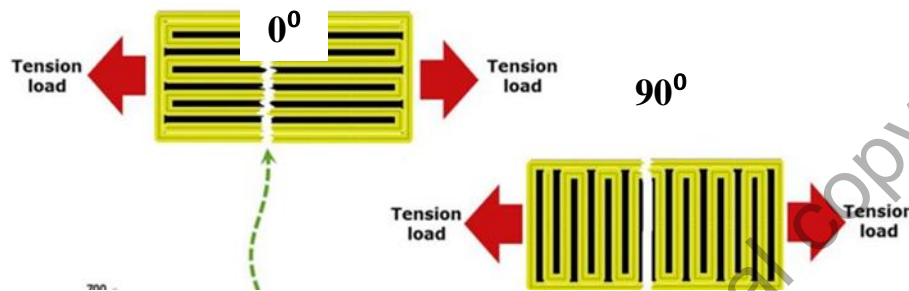


Figure 2.2 Effect of raster angle with subjected to tension load (Mohamed et al. 2016)

### 2.3.2 Effect of Infill Density on Printed Specimen

Furthermore, another important parameter is the infill density parameter. Figure 2.3 shows the infill density of the printed specimen. However, Fernandez et al. (2016) evaluated three types of infill densities namely 20%, 50%, 100% and three different infill pattern which is rectilinear, honeycomb and line. The air gap from the 3D printed object can be reduced by controlling the infill density percentage. They found that the highest tensile strength (36.4 MPa) is the combination of 100% infill density with the rectilinear pattern. On the other hand, printing orientation affects the elastic modulus of the printed part due to interlayer bonding effect. They have concluded that the infill density significantly affects the strength and stiffness of the printed specimen (Fernandez-Vicente, Calle, Ferrandiz, & Conejero, 2016; Abbas, Othman, & Ali, 2017) If the specimen printed at high infill density it might produce a solid structure compared to specimen printed at low infill density which produces porous structure (Abbas et al.,

2017). The highest compressive strength was found in specimen printed with 100 % infill density because it can stand the more compressive load due to a decrease in porosity (Domínguez-Rodríguez, Ku-Herrera, & Hernández-Pérez, 2017).

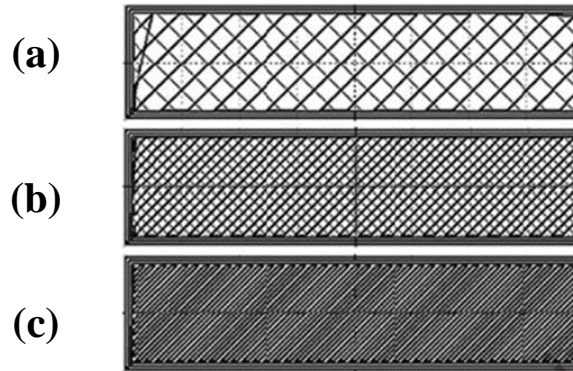


Figure 2.3 Image of different infill density; (a) 20%, (b) 50% and (c) 100% (Fernandez-Vicente et al., 2016)

#### 2.4 Conductive Polymer Composites

The conductive polymer is used in many industries, especially in the electronic and microelectronic products, for example, electronic packaging (Agrawal & Satapathy, 2014). However, the polymer is categorized as insulating material which has low thermal conductivity and is not electrically conductive (Agrawal & Satapathy, 2014). The conduction of the insulating polymer hinge on factors like; original conductivity of the polymer matrix and filler, shape and size of the filler, the content of the filler, and process fabrication of the composites (Lee & Dai, 2009).

Currently, the usage and demand for conductive polymer composites is increasing due to the high technology and advanced devices. The conductive filler is added to the insulative polymer to increase the conductivity behaviour of the base polymer. Previous

research has shown that many works have been done to improve the conductivity of the polymer, for example, a study conducted by Zhang et al. (2009), that shows the electrical conductivity of thermoplastic polyurethane increase after added with carbon nanotube (CNT) (R. Zhang, Dowden, Deng, Baxendale, & Peijs, 2009). This was supported by another research (Jin, Lin, Song, Gui, & Leesirisan, 2013) that found electrical conductivity increased by increasing conductive filler into the insulating polymer (Jin et al., 2013).

The basic idea of the conductive polymer is to be able to conduct heat or electricity. The conductive polymer can be manufactured in two ways such as by conjugating the polymer and by adding the conductive filler into the polymer. The conjugated polymer is limited to use for few thermosetting polymers only. Thus, the limitation on the types of the polymer to be used for conjugating makes the compositing technique come first.

Agrawal and Satapathy (2014), has increased the thermal conductivity of epoxy and polypropylene (PP) by adding aluminium oxide ( $\text{Al}_2\text{O}_3$ ) filler. The thermal conductivity of epoxy and PP increased up to 482% and 498% respectively. The Tg of both materials also increased from 98 °C to 116 °C for epoxy and -14.9 °C to 3.4 °C for PP. All the increment was archived after 25 vol%  $\text{Al}_2\text{O}_3$  was added into both matrix materials (Agrawal & Satapathy, 2014).

Nabilah et al. (2017) found that the addition of Carbon Nanotube (CNT) and Carbon Fiber (CF) as a secondary filler to epoxy increased the through-plane conductivity to 40.3 S/cm and 19.9 S/cm respectively. This result has proved that by adding conductive

filler into an insulative polymer, the electrical conductivity has increased due to the formation of the conductive network by the fillers. Also, there was a 24% increase in flexural strength of CF/EP when added with CNT while almost 9% increase in flexural strength when added with CB as a secondary filler due to good filler dispersion. Moreover, when the filler loading increased, the filler tends to fill the void of the matrix, resulting in the reduction of void content (Nabilah et al., 2017).

Liang and Tjong (2007) found that the electrical conductivity of the Low Density Polyethylene (LDPE) increases gradually by increasing Aluminium (Al) and Multiwall Nanotube (MWNT) filler. This is due to the formation of conductive pathways from the filler connection (Liang & Tjong, 2007).

However, in some application of conductive polymer composites, for example for top globe encapsulation, they acquire the high conductivity for thermal only but not for electrical conductivity. Therefore, thermally conductive but electrically insulative polymer composites is the alternative material that match to the application.

#### **2.4.1 Thermally Conductive but Electrically Insulative Polymer**

The advantages of thermally conductive but electrically insulative polymer are lightweight, low cost, ease of machining and forming, resistance to corrosion, good capability of high production rate, low cost, low electrical conductivity, good rigidity for mechanical hardness and good thermal stability (Makled et al., 2005; Essabir et al., 2017).

Because of the unique ability of thermally conductive but electrically insulative polymer composites, many studies have been done to improve the properties of polymer-based on the application requirement. Essabir et al. (2017) studied the effect of iron oxide ( $\text{Fe}_3\text{O}_4$ ) on the ABS/PA6/SBR blends prepared using a twin-screw extruder. They found that Young's modulus increased with increasing  $\text{Fe}_3\text{O}_4$  loading due to the high specific rigidity of the filler. Good filler dispersion and distribution and filler-matrix interaction also contributed to the increase in Young's modulus. Besides, the complex modulus ( $G^*$ ) also increase with  $\text{Fe}_3\text{O}_4$  loading due to the presence of rigid particles that limits the polymer chain movement. The electrical conductivity experienced a slight increase when the filler concentration increased due to the interconnection between filler particles to form conductive passage which indicates to the electrical flow with high surface resistance (Essabir et al., 2017).

## **2.5 Thermally Conductive but Electrically Insulative Filler**

Fabricating conductive polymer required high conductivity filler to be incorporated with insulative nature of the polymer. There are three types of conductive filler traditionally used in constructing conductive polymer like carbon-based filler, metallic filler and ceramic filler (Ngo, Jeon, & Byon, 2016). The carbon-based filler is known as the most ideal filler for high thermal conductivity (Ngo et al., 2016). However, in fabricating conductive polymer by introducing a carbon-based filler, it is required a high amount of filler, within 60 wt% – 80 wt% (Nabilah et al., 2017). Nevertheless, the high amount of filler promotes poor mechanical properties (Nabilah et al., 2017) to the composites system. Another good conductive filler was metallic filler which offers high thermal and electrical conductivity. However, metallic filler gives higher thermal

expansion compared to other fillers like carbon and ceramic (Ngo et al., 2016). Besides, ceramic can be an alternative way to fabricating a conductive polymer compared to carbon and metallic filler. In addition, ceramic fillers offer unique properties to the matrix base. For example, ceramic provides good dielectric properties and thermal conductivity and good thermal stability. Otherwise, ceramic ferrite promotes low electrical conductivity to the specimen.

The drawbacks found that several fillers might increase the conductivity of the polymer thermally or electrically such as metal-based filler, fibre-based filler, and carbon-based filler. However, in some application that requires thermally conductive but electrically insulative may not suit those fillers. Therefore, a ceramic-based filler may suit to the required application, for example, ceramic ferrite filler or metal oxide filler. Previous findings proved that ceramic ferrite filler possesses good thermal conductivity and remain low in electrical conductivity.

Ceramic ferrite also was known as a magnetic material due to the ability as a ferrimagnetic material (Rekošová, Dosoudil, Ušáková, Ušák, & Hudec, 2013). Ceramic ferrite is a functional material (Essabir et al., 2017) that has unique advantages include high initial permeability, electrical resistivity and low magnetic, dielectric loss (Rekošová et al., 2013), low cost and good chemical resistant (Soloman, Kurian, Anantharaman, & Joy, 2004).

Ceramic filler can be synthesized in many methods and one of them was a ceramic method or solid-state method. Ceramic methods or solid-state method were done by heating the mixture of metal oxide powder at a certain temperature and at a certain

holding time (Etourneau, 1999). Most researchers preferred using ceramic methods than other methods because easier, less harmful and more environmentally friendly because using less chemical and low sintering temperature.

For example, Hankare et al. (2010), were trying to synthesize  $\text{CuZnFe}_2\text{O}_4$  using oxalate coprecipitation method. Stoichiometrically,  $\text{Cu}_{1-x}\text{Zn}_x\text{Fe}_2\text{O}_4$  with  $x = 0.0, 0.25, 0.5, 0.75$  and  $1.0$  were used in this study. It starts by preparing oxide metal via oxalate co-precipitation method. The prepared compound then was undergoing drying process at  $110^\circ\text{C}$  and sintered at  $900^\circ\text{C}$  for 6 hours. The prepared sintered powder was pressed into pellets shape after added with 2% of polyvinyl alcohol and heated again at  $773\text{K}$  to remove the organic binding agent. In this study, they have analysed the magnetic properties of copper ferrite when substituted with zinc. Results taken from x-ray diffraction shows that all specimen successfully formed in a single cubic phase. The lattice parameter had increased when zinc content increased due to the ionic radius of  $\text{Cu}^{2+}$  are smaller than  $\text{Zn}^{2+}$ . The results obtained from scanning electron microscopy also shows that the average ferrite's grain size increase until reach  $x = 0.5$  and decrease back with further increase in  $x$ . The image also shows increasing in grain size will decrease the porosity. The study also had performed the X-ray spectroscopy to study the composition. The result shows that no impurities found in the observed spectra which indicate that no reaction happened of the cation impurities (Hankare, Kadam, Patil, Garadkar, Sasikala, & Tripathi, 2010).

Bukhal et al. (2014) had synthesized copper substituted cobalt zinc ferrite using sol-gel auto combustion method. In this study, they have performed the substitution based on the  $\text{Co}_{0.6}\text{Zn}_{0.4}\text{Cu}_x\text{Fe}_{2-x}\text{O}_4$  stoichiometry where  $x=0.2, 0.4, 0.6, 0.8$  and  $1.0$ . The X-ray

diffraction results show that peak intensities of  $\text{Co}_{0.6}\text{Zn}_{0.4}\text{Cu}_x\text{Fe}_{2-x}\text{O}_4$  have increased with increase in annealing temperature at approximately 400 °C to 1000 °C. This indicates that the improvement of crystallinity was due to the increase in the crystalline volume ratio of the nuclei and increases in the size of the particle. About 40 to 60 nm of average crystallite size was recorded have been used in this study. Besides, the increase in copper concentration in  $\text{Co}_{0.6}\text{Zn}_{0.4}\text{Cu}_x\text{Fe}_{2-x}\text{O}_4$  might increase the lattice parameter due to the larger ionic radius of copper (0.73Å) then the ionic radius of iron (0.67Å). The same pattern also shows that the x-ray density where the increase in copper concentration may increase the behaviour of  $\text{Co}_{0.6}\text{Zn}_{0.4}\text{Cu}_x\text{Fe}_{2-x}\text{O}_4$  because of the higher atomic mass of copper rather than the atomic mass of iron. The bond length of  $\text{Co}_{0.6}\text{Zn}_{0.4}\text{Cu}_x\text{Fe}_{2-x}\text{O}_4$  has shown an increase when the concentration of  $\text{Cu}^{2+}$  increase attributed to the increase in lattice constant in the ferrite specimen. The electrical resistivity testing that has been performed on the specimen using the two-point probe has revealed that all specimen tested was in semiconductor nature of the nano ferrite. They have explained the conduction mechanism using the basis of Verwey de Boer mechanism, which encompasses electron exchange between element with more than one valence state in the equivalent sites in the lattice. N-types belongs to  $\text{Fe}^{2+} \leftrightarrow \text{Fe}^{3+}$  while  $\text{Cu}^{2+} \leftrightarrow \text{Cu}^+$  give p-type. In this case, the existence of copper substitute cobalt zinc ferrite,  $\text{Fe}^{3+}$  ions are replaced by  $\text{Cu}^{2+}$  ions led to reducing the formation of  $\text{Fe}^{2+}$ . Hence, ferrite becomes p-type conduction due to jumping between  $\text{Cu}^{2+} \leftrightarrow \text{Cu}^+$ . This situation may be due to electron jumping between  $\text{Fe}^{2+} \leftrightarrow \text{Fe}^{3+}$  and  $\text{Cu}^{2+} \leftrightarrow \text{Cu}^+$ . The results of electrical resistivity show that linear decrease recorded when increasing in temperature which may mean that semiconductor nature of the tested specimen. Increasing temperature leads to an increase in the drift mobility of thermally activated charge carrier as well as electron jumping. They have summarized this result as, when the unit cell parameter increases

linearly with the increase in the concentration of Cu, the ionic radius of Cu is bigger than the ionic radius of Fe. Besides, the D.C. electrical conductivity decreases upon the increase in the temperature which might create semiconductor nature of the specimen (Bhukal, Shivali, & Singhal, 2014).

Bardhan et al. (2010) synthesized zinc ferrite nanoparticle at low temperature using a solid-state method. The x-ray diffraction result shows that all peaks belong to spinel zinc ferrite without the presence of zinc oxide or iron oxide. This result indicates that the pure formation of zinc ferrite was obtained. They found that the zinc ferrite nanoparticles were increased with increasing annealing temperature. The result shows that about ~20 -25 nm grains are formed. The chemical characterization was done using x-ray photoelectron spectroscopy and found that Fe presence in both  $\text{Fe}^{+2}$  and  $\text{Fe}^{+3}$  states. The ratio of  $\text{Fe}^{+2}/\text{Fe}^{+3}$  increased by decreasing the temperature whereas when the temperature increased, the  $\text{Fe}^{+3}$  states were more stable compared to  $\text{Fe}^{+2}$  states. They have mentioned that zinc ferrite in bulk condition displays spinel structure with  $\text{Zn}^{+2}$  ion present in tetrahedral sites while  $\text{Fe}^{+3}$  resides in octahedral sites. They also found that the increase in temperature has increased the concentration of  $\text{Fe}^{+2}$ . Bardhan concluded that the decrease in temperature might increase the strain resultant to reduce the particle size. The ionic radius of  $\text{Zn}^{+2}$  is smaller (0.74 Å) compared to the  $\text{Fe}^{+2}$  (0.77 Å). Hence, the increase in strain may be due to the substitution of  $\text{Zn}^{+2}$  by  $\text{Fe}^{+2}$  at tetrahedral sites. Finally, they concluded that the heat treatment temperature increases the ratio of ferric to ferrous ions increase laterally increase zinc ferrite particles size (Bardhan et al., 2010).

Barba et al. (2017) used  $(\text{Cu}_{0.12}\text{Ni}_{0.23}\text{Zn}_{0.65})\text{Fe}_2\text{O}_4$  pressed in cylindrical and toroidal shape using uniaxial dry pressing at 300 MPa compaction pressure. The prepared